BEARINGLESS MAIN ROTOR HUB CONCEPT USING PRECURED CARBON FIBRE RODS IN A FLEXIBLE MATRIX

K.D. Potter & M.R. Wisnom
Department of Aerospace Engineering, University of Bristol.
Queen's Building, University Walk, Bristol. BS81TR. UK.

Abstract

Bearingless rotor hubs have been developed for some small helicopters and for tail rotors. To date it has proven very difficult to develop a bearingless hub for the main rotor of a heavy helicopter. This paper discusses an approach to the development of such hubs, based on the use of precured carbon fibre rods in a flexible matrix to produce a flexbeam. The paper considers the required properties in such a matrix, describes the work to formulate such a matrix and the properties of samples of rods embedded in that matrix, and goes on to describe the design, manufacture and test of a sub-scale prototype.

Nomenclature

a	Half width of sample
b	Half thickness of sample
d	eccentricity
DGEBA	Diglycidal ether of bisphenol A
G	Shear modulus
K	Torsion constant
L	Sample length
M	Bending moment
R	Rotation, in radians
T	Torque
T_g	Glass transition temperature
TETA	Triethylene tetramine

Introduction

Bearingless rotor hubs have been developed for some small helicopters and for tail rotors, refs 1-8. To date it has proven very difficult to develop a bearingless hub for the main rotor of a heavy helicopter. Such rotor hubs have been made, using composite materials in a complex cross section to achieve the required relatively low torsional stiffness and relatively high bending stiffnesses, see fig 1.

However, the working sections of such solutions tend to be of a greater length than would be ideal. Additionally the necessary complex cross sections have proven very difficult to manufacture to a reliable quality, especially in the regions where the complex cross section must blend out into a more prismatic shape. An alternative design would be to utilise a low stiffness matrix resin with conventional fibre reinforcement. However, this design approach leads to a very limited compressive strength, which is unable to meet the loading requirements for the main rotor hub of a heavy helicopter.

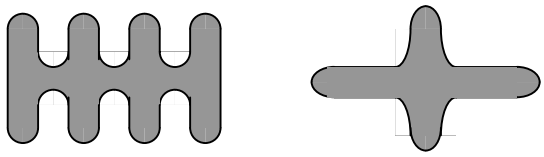

Fig 1. Geometries that can be used to minimise torsional rigidity in components that are stiff in bending.

Work at Bristol University in collaboration with Agusta Westland has explored a third option, which looks very promising. The approach taken has been to utilise small diameter rods of pre-cured carbon fibre material embedded in a specially formulated flexible matrix. The rods have very high compressive performance, due in part to their having extremely straight fibres, ref 9. The innate resistance of the rods to bending means that a much lower embedding modulus is required to support the rods against buckling than would be the case for conventional fibrous reinforcement. This factor then opens up the design space and allows the balance of properties required for a bearingless main rotor to be approached.

The work proceeded in three stages towards the production of a sub-scale demonstration component embodying many of the features needed in a functional bearingless main rotor. The first stage was to use finite element modelling to identify the mechanical properties required in the embedding matrix such that a low torsional stiffness could be achieved at the same time as adequate longitudinal compressive strength. The second stage was the formulation of a matrix material of the target properties, and the manufacture of test coupons to allow the mechanical performance of the combined rod/matrix structures to be assessed and verify the predictions of the finite element modelling. Alternative methods of achieving the required balance of properties were also studied in this part of the programme. The last stage was to design a sub-scale demonstrator to permit the torsional

stiffness to be measured at a more representative scale.

Finite element analysis.

A suitable set of loads and required torsional, flap and lag stiffnesses were provided by Agusta Westland, based on previous work using conventional composite materials in a complex cross-section. Hand calculations were used to define a preliminary geometry for a flexbeam, using the data noted above and estimated properties for carbon fibre rods in a flexible matrix. It was quickly found that a fully representative 3D FE model of that flexbeam geometry would require several million elements if the individual reinforcement rods were to be modelled. At the other extreme, using homogenised orthotropic material properties, not including the bending stiffness of the rods, resulted in a prediction of local microbuckling at relatively low flexural stress levels, as would be expected. Thus it was necessary to develop a practical analytical technique for such structures.

The development started with simple 2D plane stress analyses of rectangular, longitudinal sections through the flexbeam. In these models individual rods could be represented and assessment could be made of the stiffness and stress distribution. Critically, the buckling stability in the depthwise sense could be established. Three dimensional thin slice models, also incorporating one layer of individual rod elements were then created to look at buckling stability including the effects of chordwise deformation. Small-scale constant beam sections with relatively small numbers of rods were then analysed to investigate material torsional stiffness and flexural/torsional buckling characteristics.

Subsequently, an investigation into 'lumping' together groups of rods was carried out on the 2D models in order to reduce the number of elements and give a practical approach to the analysis of a fully representative 3D model. A full scale model of the flexbeam was then created using this "lumped rod" technique. The analyses included geometrically non-linear (large deflection) analyses as well as linear static and linear buckling models. All analyses used linear material properties. As the analysis was being carried out in part to set the matrix property requirements no experimental data on non-linear material properties was available. The developed models were then used to predict the performance of both prismatic test specimens and a sub-scale demonstrator component. See fig 2, which shows the predicted shapes for pin-ended compression of a prismatic sample with an elastomeric matrix.

This work gave limiting values for the properties of the embedding matrix as a modulus of no less than 130MPa to provide adequate support to the rods and permit them to carry at least 1GPa in compression without buckling, and no more than 370MPa to give a torsional stiffness below the required limiting value.

Material Requirements

In order to provide a baseline for experimental and analytical work a single reinforcing rod type was selected. This was a 1.7mm diameter carbon fibre (IM7) reinforced rod commercially available under the trade name Graphlite. This rod is very straight and has excellent mechanical properties as shown in table 1, refs 9, 10.

Test mode	Ultimate strength GPa	Strain to failure %	0.4% secant E GPa
Axial tensile	3.06	1.49	196
Axial compression	1.84	1.04	175

Table 1. Basic mechanical properties of the carbon fibre rods

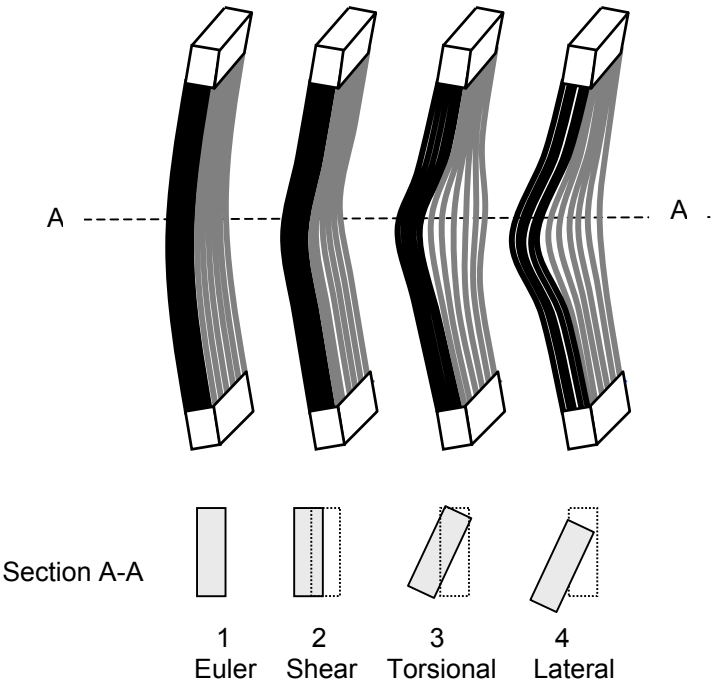

Fig 2. The predicted first 4 buckling modes of polyurethane matrix samples.

Matrix Formulation

Matrix formulation was carried out against a set of requirement statements for mechanical, physical, environmental resistance and manufacturing properties. These requirement statements are laid out below.

Ideal property requirements

- Shear modulus between 45 & 130MPa, (equating to tensile modulus between 130 & 370MPa at a Poisson's ratio of 0.45)
- Minimum shear strength above 10MPa, based on shear stress at limit load in the region of 6MPa.
- Operating temperature range -50^0 $+70^0$C
- No thermodynamic transitions in this range (e.g. the glass transition temperature, T_g)
- Constant mechanical properties over the operating temperature range
- Constant mechanical properties over the operating strain range and strain rate range
- Resistant to attack from water, salt spray, lubricating and hydraulic oils, fuel, de-icer, common solvents etc.
- Minimal change in mechanical properties as a result of moisture or other fluids uptake
- Resistant to creep, fatigue and stress rupture
- Available in a curable liquid, paste or film form for fabrication purposes
- High bond strength to pre-cured carbon fibre rods rods (No exact value available, but the bond strength between matrix and pre-cured carbon fibre rods should not be the limiting factor in element shear or transverse strength)
- Durable bond strength to pre-cured carbon fibre rods
- Coefficient of thermal expansion compatible with pre-cured carbon fibre rods ($\approx$ 0 axially and $\approx$ 30E-6K^{-1} radially) and with end fitting metals if bonded end joints used (e.g. $\approx$ 9E-6K^{-1} for titanium)
- Bulk modulus should be in the same range as tensile modulus; to avoid non-linear responses due to any hydrostatic stresses which might arise in some stressing modes and to minimise thermal stresses under constraint such as might be seen at bonded metallic end joints.

An extensive search for materials that could meet this set of requirements proved to be unsuccessful. Realistically, some of these target properties cannot be expected to be met, for example the ideal matrix thermal expansion characteristics. However, it was felt useful to have such a set of property requirements against which the achievable matrix properties could be set.

The most critical requirements are the first four, which set the stiffness and strength requirements, the operating temperature range and require a T_g outside the operational temperature range. This last requirement can be relaxed somewhat to a requirement that the stiffness requirements are met at all combinations of temperature and environmental conditions. However, the target stiffness range is essentially that of polymeric materials in the region of their T_g. The modulus of, for example, an epoxy resin would be expected to vary by up to two orders of magnitude across its T_g, making it very unlikely that material properties will be sufficiently stable in the region of T_g. Two formulation approaches were taken, firstly to generate a material with a T_g above the operational temperature range and the other to generate a material with a T_g below the operational temperature range.

A T_g above the operating temperature can best be obtained by making a syntactic foam with a suitable polymer and experiments were carried out with a DGEBA epoxy and TETA hardener. This material had a Young's modulus of about 3GPa. It was found that in order to achieve a modulus in the required range a porosity of more than 75% would be needed. A bimodal distribution of polymeric microspheres and macrospheres (expanded polystyrene) achieved a porosity of 74% and a Young's modulus of 400MPa. The bulk modulus would be expected to be acceptable due to the high level of porosity. However, the strain to failure was only 0.4% and the mixed uncured syntactic was very viscous and would be difficult to incorporate in practical mouldings.

A Tg below the operating temperature can best be achieved by filling a suitable elastomer. A two part polyurethane elastomer of 94Shore A hardness was taken as a baseline. This material had a Young's modulus of about 65MPa. Adding alumina grit to this polyurethane, at 150 parts by weight to 100 parts by weight of elastomer, gave a 1% secant modulus of 150MPa, with a tangent modulus falling to 100MPa at 1% strain, although the properties showed more non-linearity than the baseline polyurethane. A relatively coarse grit of alumina (up to 100μm) was used to avoid an excessive viscosity rise. Even so this formulation was very viscous and would be difficult to incorporate in practical mouldings. Equally, the bulk modulus would be expected to be high and the addition of polymeric microspheres (as well as alumina) to limit the bulk modulus led to the Young's modulus falling back to the level of the unfilled elastomer.

Neither of the two formulation approaches gave a material that would be fully suitable as an embedding matrix with regard to either mechanical or manufacturing properties.

A final approach brought together the first two approaches in that the epoxy and polyurethane elastomer were combined. Cured and powdered (very irregularly shaped particles with a 20-100μm particle size) polyurethane was mixed into the uncured epoxy at 40% by volume polyurethane. This formulation was much stiffer than required at 850MPa, but it was far more robust than either of the other material types.

The conclusions of this work on formulating an embedding matrix were:

- The production of a very low density syntactic foam can give a combination of high T_g and a stiffness which is just acceptable, but obtaining an adequate strain to failure and strength appears to be much more difficult
- The production of a heavily filled polyurethane elastomer can give a combination of a low T_g and a stiffness that is just acceptable, but with a high bulk modulus
- Blending a solid elastomer crumb with an uncured epoxy gives a very robust material but of an excessive stiffness.
- All the above approaches produce a material that would be difficult to utilise for manufacturing due to excessive viscosity.

It is believed that the first approach would prove intractable and that the other approaches have more technical merit, however, the manufacturing properties of any of these formulation approaches are seen as very negative.

For these reasons the effort to formulate an embedding matrix of the correct properties was closed and the work continued in two new directions. The first was to concentrate on formulating a matrix of the correct mechanical and manufacturing properties at room temperature to validate the FE modelling. The second was to investigate the possibilities for using an elastomeric matrix and providing additional reinforcement directions to stabilise the structure against the identified buckling modes.

A formulation with suitable properties and with adequate pot life for the manufacture of small, prismatic specimens was arrived at by blending a blocked polyurethane (Trixene B1770, Baxenden Chemicals) with a DGEGA epoxy and TETA hardener in the proportions 104g epoxy to 96g polyurethane to 15g hardener. The system was mixed under vacuum at 40C, cast into a mould tool and cured. The modulus of this blend was found to be 500MPa at 20C, which was slightly above the target level, although the modulus reduced to 270MPa at 50C. A lower modulus could have been achieved with a higher polyurethane loading, but this would have had a higher uncured viscosity, which would have been negative from a processing viewpoint. As the intent was to validate the FEA this formulation was used for initial trials work.

To investigate the second approach, samples were made up with a polyurethane elastomer matrix and a small amount of aramid fibre was wound around the sample at +/-45^0. A single tow of 1140Den aramid fibre was used, wound at +/-45^0 on a pitch of 8mm and impregnated with resin. This was estimated to give a torsional stiffness similar to that of the PU-epoxy blend sample. These samples were only tested for their buckling resistance in pin-ended compression. If this approach proved to be valid it would be expected that the torsional buckling mode illustrated in fig 2 would be suppressed, although the other buckling modes would be unaffected. Additional reinforcement directions would be needed to eliminate the other buckling modes.

Manufacture and testing of prismatic samples

Sample manufacture

Samples were made at nominal dimensions of 10mm thick, 28mm wide and 360mm long. The reinforcement consisted of 6 layers of 13x 1.7mm diameter rods. The spacing between the rods was maintained using a very light interweaving of 0.2mm diameter nylon monofilament. The epoxy/polyurethane mix was introduced by a resin transfer moulding technique. Similar samples were made up using a polyurethane elastomer of 94Shore A hardness (Devcon Flexane liquid 94) and the DGEBA/TETA epoxy.

Sample testing

The samples were tested in three ways, torsion, bending and pin-ended compression.

Torsion testing was carried out using an Avery-Denison torsion machine type 6609 CGG. The end fittings used were simple rectangular slots into which the sample was pushed. The sample was a slide fit in the end grips and was shimmed with PTFE coated glass cloth to give a good fit whilst avoiding clamping against warping deflections at the grips.

The modulus, G, was calculated in each sample with the formula shown below:

$$G = TL/KR \qquad (2)$$

Where T = Torque; L = Length between clamps; R = Rotation in radians (Twist), K is the torsion constant..

$$K = ab^3[16/3 - 3.36b/a(1-b^4/12a^4)] \quad (3)$$

Where 2a = width of the sample; 2b = thickness of the sample.

The results of this testing are shown in table 2.

Matrix material	G MPa
Epoxy	2900
Epoxy / PU	807
PU	117

Table 2. Shear moduli for various matrices

One epoxy matrix sample was tested to destruction. It failed at a load of 58Nm (which for an isotropic material would equate to a shear stress of 72MPa) and a twist of 29^0. Failure was by cracking at 45^0 at the midpoint of the specimen. The polyurethane matrix specimens could not be failed, at a twist of 60^0 the test was stopped due to concerns about the samples coming out of the grips. When the load was removed the sample snapped back to its undeformed shape.

Bending tests were primarily carried out at low loads in order to establish the bending modulus rather than the strength of specimens. Tests were carried out on a Instron 1341 servohydraulic machine under three-point bending conditions.

The results of the testing are shown in table 3. For each sample a tensile modulus was estimated on the basis of the rod modulus and the Volume Fraction of rods for that specimen, this figure is also quoted in table 3.

Matrix material	Flexural Modulus GPa	Tensile Modulus GPa
Epoxy	93	113
Epoxy / PU	87	105
PU	28	108

Table 3. Results from flexural testing

The epoxy and epoxy /PU specimens both showed flexural moduli of about 17% less than that predicted on the basis of the rod stiffness in the absence of shear deformation.

A developmental video metrology equipment (ref 11) was used to investigate this further for the epoxy / PU matrix sample. The video metrology equipment can accurately track the position of features in a video stream and provide XY data on the centres of the features. This data stream can then be used to identify angles and other features of value. Figure 3 shows the set-up used in this case. Three target spots were painted on one end of the specimen, supported in a three point bend test rig.

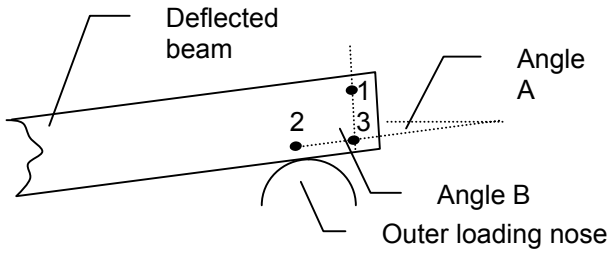

Figure 3. Set-up for video metrology

The angle between points 1 & 3 and the vertical plane and between points 1 & 2 and the horizontal plane were monitored by the video metrology equipment during the test. Pure bending would lead to angle B remaining unchanged as angle A changes. Pure shear would lead to the change in angle B being equal to that in angle A. The measured relationship between angles A and B is shown in Fig 4, over four cycles of loading and unloading.

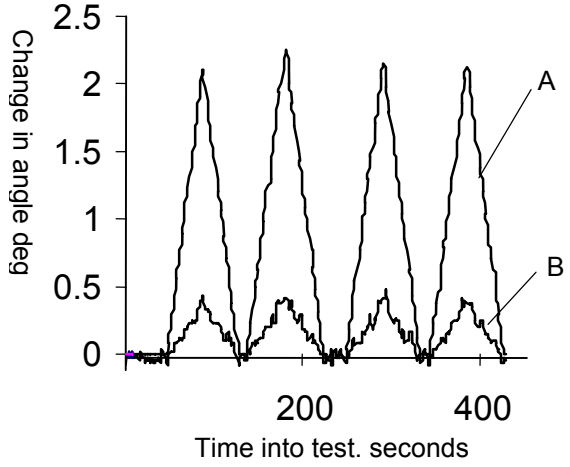

Fig 4. Results of video metrology

Quite a lot of scatter can be seen on the trace for angle B, this is not really surprising for the measurement of such small angles during a live test. Averaging for the four cycles the B angle change was 21% of the A angle change and 17% of the total A+B angular change. This agrees well with the finding that the flexural modulus was 17% less than that predicted on the assumption of pure bending.

As the bending test progressed the shear contribution increased until at failure shear was the

dominant deformation mode. Post-test examination of the failed specimen showed that failure occurred by extensive shearing between the layers of carbon/epoxy reinforcing rods without crack initiation.

Table 4 lays out the results from the testing of the embedded rod samples in terms of the ratios of torsional, bending and tensile moduli for the three sample types.

Matrix material	Torsion / Flex / Tensile modulus ratio
Epoxy	1 : 32 : 39
Epoxy / PU	1 : 108 : 130
PU	1 : 239 : 923

Table 4. Modulus ratios for three sample types

The epoxy matrix sample gave results for the modulus ratios in line with expectations for a rigid matrix laminate. The polyurethane matrix samples demonstrated extraordinarily high modulus ratios, which may have use in other applications, but would be excessive in the context of bearingless main rotor flexbeam. The epoxy / PU matrix samples show modulus ratios in the required region.

Pin ended compression tests were carried out to check the predictions of FEA with respect to the buckling modes of these samples.

Fig 5 shows the principle of operation of the pin-ended compression rig.

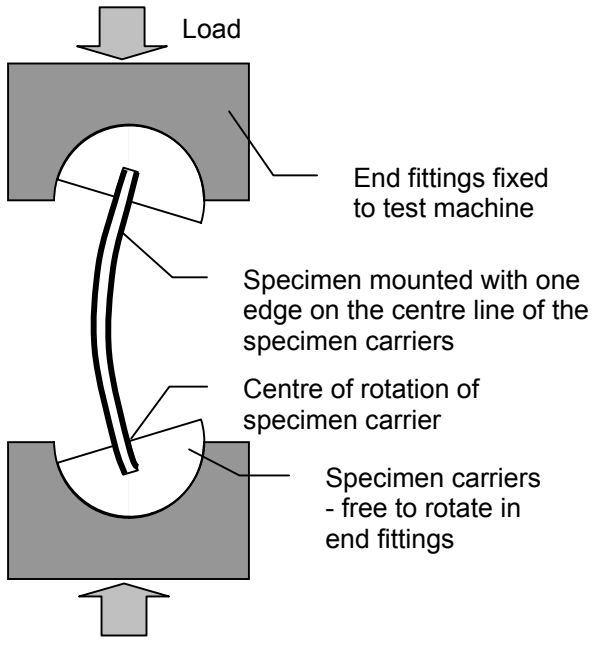

Fig 5. Schematic of pin-ended compression rig

PTFE shims are mounted between the end fittings and the specimen carriers to minimise the resistance to rotation. As the specimen is off-centre in the specimen carrier, bending and a lateral deflection of the sample occurs immediately that any displacement is applied. Steel shims are used between the specimen and the specimen carrier (on the specimen's tensile face) to ensure a good fit.

A video camera was set up in order to take pictures of the sample shape. A white line was drawn on the middle of the sample and pictures were taken at every 1 mm cross-head displacement. The Image-Pro Plus software was used to measure the eccentricity (d) of the sample from these pictures. The eccentricity was taken as the distance from the midpoint of the specimen to a line drawn between the centres of rotation of the end pieces. See fig 5 for the position of the centre of rotation. The eccentricity is required in the calculation of the bending moment imposed on the specimen.

$$M = W.d \qquad (4)$$

Where M is the bending moment, W is the applied load and d is the eccentricity.

From the load data from the test machine and the eccentricity data the bending moment and end load can be used to estimate the rod stress due to bending, to which must be added the compressive end load to give the maximum compressive stress carried by the rods.

A load versus bending moment curve for an epoxy matrix samples is shown in fig 6.

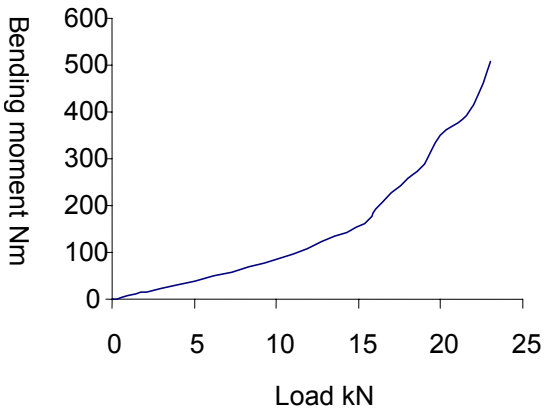

Fig 6. Load versus bending moment for an epoxy matrix specimen tested in pin-ended compression.

The deviations from a smooth curve in fig 6 are believed to be due to the method of measuring the sample's eccentricity.

This epoxy matrix sample failed catastrophically by shear of the embedding matrix, although some of the carbon fibre reinforcing rods were also damaged. At the point of matrix failure the peak compressive stress in the rods was estimated at 1.7GPa. No buckling modes were seen other than overall Euler buckling.

For the epoxy / PU matrix samples a peak was seen in the load / deflection curve and in the load versus bending moment curve as shown in fig 7. Strain gauges were also fixed at the points of peak tensile and compressive strains for one sample as a cross-check of the calculations based on bending moment. Fig 8 shows the measured strain versus bending moment curves. The peak compressive strain based on the bending moment calculation was 1%, which was in good agreement with the measured peak compressive strain.

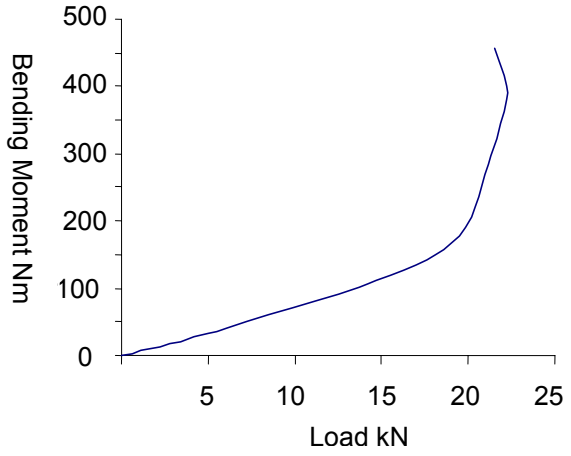

Fig 7. Load versus bending moment for an epoxy / PU matrix specimen tested in pin-ended compression.

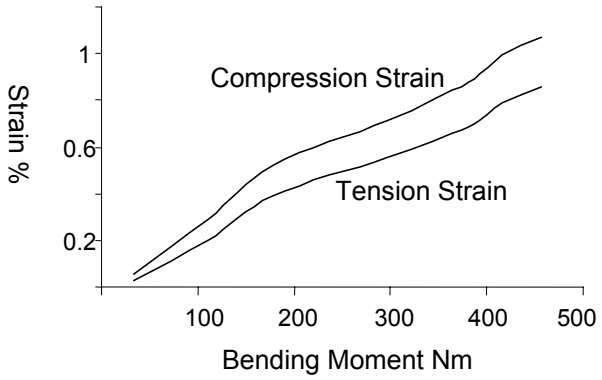

Fig 8. Surface strain versus bending moment for an epoxy / PU matrix specimen tested in pin-ended compression.

The deviations from smooth curves in figs 7 & 8 are, as before, believed to be due to the method of measuring the sample's eccentricity.

This epoxy / PU matrix sample failed by shear cracking in the embedding matrix, however the failure was much less dramatic than that experienced by the epoxy matrix samples without any failures in the reinforcing rods. No buckling modes were seen other than overall Euler buckling.

For the polyurethane matrix samples the load peaked at around 2mm end deflection, compared to around 6mm for the samples with stiffer matrices. Peak load varied in the range of 7.5 to 8.5kN, both between samples and for the same sample under repeat testing. The buckling behaviour was, as expected, much more complex. The shear buckling mode shown in fig 2 was initiated from a very low load, the load continued to rise after shear buckling was initiated. Just after peak load the torsional buckling mode was initiated, coupled with a 2kN load drop, the load continued to drop as the lateral mode became apparent. There was no sudden onset of any of the buckling modes. The final buckled shape was very complex having characteristics of all three buckling modes. Due to the global buckling seen in these samples no attempt has been made to estimate rod stresses. In general terms, complex buckling modes are displayed at about 30% of the loads that can be sustained by either the PU-epoxy blend or unmodified epoxy samples. On the other hand these samples are extraordinarily robust with regard to recovery without damage from some very contorted buckling states, which must impose high local shear strains on the matrix. The samples were repeatedly deformed into severely buckled shapes with no indication of any damage or permanent set.

As noted above, polyurethane matrix samples were prepared that had been lightly overwound with aramid fibres at $+/-45^0$ in an attempt to suppress the torsional buckling mode. The first specimen had a peak load of 9.5kN, and the torsional and lateral buckling modes appeared to be completely suppressed, even at a very extreme case of a 15mm end displacement (compared to the 6mm deflection at failure for the epoxy matrix specimen). However, the shear deformation between the layers of reinforcing rods clearly dominated the overall deformation, this deformation mode becoming apparent between 1 and 1.5mm of end displacement. After that point the specimen was only in contact with the specimen carrier along the leading edge of the specimen, due to the shear, with a clear gap between the end of the specimen and the carrier at the trailing edge.

Another specimen was made up in an attempt to keep the ends of the specimen in contact with the specimen carrier throughout the test. At the ends of the specimen the rods were embedded in a rigid filled epoxy resin rather than polyurethane elastomer to inhibit shear between the layers of rods. The rest of the specimen was impregnated with the polyurethane and the cured specimen was overwound with aramid fibres as before. This sample exhibited a peak load of 11kN. In this case the specimen ends remained in complete contact with the specimen carriers throughout the test. However, the shear deformation buckling mode as shown in fig 2 was clearly in evidence at the peak in the load deflection curve, at about 3mm end displacement.

This activity of manufacturing and testing simple samples demonstrated that the samples behaved as would be expected from the FE analysis. The low modulus embedding matrix permitted the rods to buckle at relatively low end loads, whereas the higher modulus embedding matrices provided adequate support to eliminate buckling modes other than overall Euler buckling. It was demonstrated that composites of a very high level of anisotropy could be developed, and that the torsion / tension modulus ratio determined by FEA to be necessary for a bearingless main rotor could be achieved. However, it proved impossible within the formulation work carried out and reported here to generate a material that would have the full suite of correct properties. Initial experiments in which a small amount of oriented aramid fibre were added to a sample with a low modulus embedding matrix proved the concept of selective elimination of specific buckling modes, and gave very robust samples.

It was determined, on the basis of the results from this activity to proceed to the manufacture of a sub-scale flexbeam.

Manufacture and Test of Prototype Components

The test component was a sub-scale prototype, comprised of two end sections where the rods are terminated and an active section, where most of the deformation is expected to occur.

Active section design

The cross-section of the working section was chosen to be 50mm wide by 22mm deep, with the volume fraction of 1.7mm diameter rods chosen to be in the region of 70%. The total number of rods was selected as 332 (i.e. 7 rows of 26 rods + 6 rows of 25 rods) as shown in fig 9.

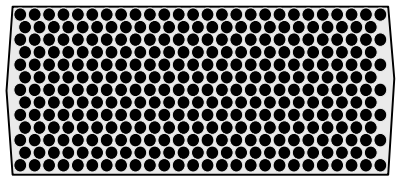

Fig 9. Cross-section of rods in the working section.

Termination design

Previous work (Ref 9) had demonstrated that the full strength of the rods could be achieved in a rod to metal adhesive bonded joint of 50mm length, using a bond thickness of about 0.6mm. To achieve such a joint for each rod requires that an array of holes is drilled in a block of metal at a regular spacing. It would be expected that a production termination would be manufactured from titanium, however for this prototype, aluminium alloy was chosen as a more suitable material. A hexagonal array of holes was drilled in a block of aluminium, with a 4mm pitch between each hole in a row and a 3.5mm pitch between rows, see fig 10.

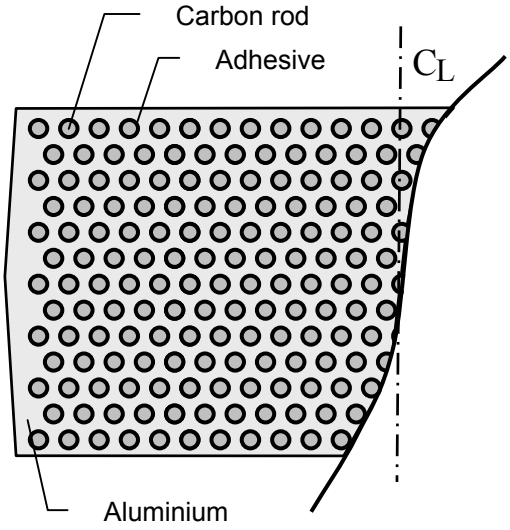

Fig 10. Arrangement of rods in the termination section. (Note, figs 9 and 10 are at the same scale)

The last 5mm of each hole was drilled at a smaller size to provide a location for the rod to ensure that the rod stays central in the bonded joint. Lastly, a draft angle of 3^0 was used from a mid-plane parting line to ensure that the moulding could be removed from the tooling in which it was made. The end fitting so designed was 104mm wide and 46mm deep. Therefore the outer rods would follow a curved trajectory from one end fitting, in to the working section, and out again to the other end fitting. Setting the worst case strain due to this bending at about 10% of the strain capacity of the

rods enabled the overall length of the demonstrator to be set at 700mm, see fig 11.

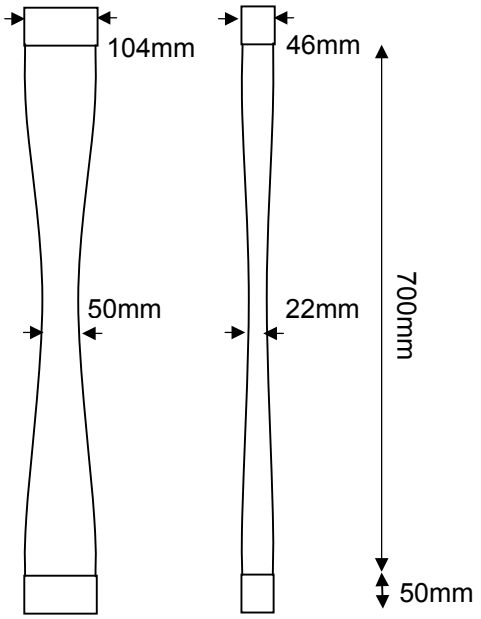

Fig 11. Overall dimensions of demonstrator component

Assembly of rods

A jig was manufactured to hold the rods in each layer in the correct position close to the end fittings. This was simply made from an aluminium bar with slots cut on an appropriate pitch. In addition, it was necessary to ensure that each rod had the correct trajectory, and hence position, in the working section. This was achieved by weaving a tow of aramid fibre around the rods of each layer. It was intended to introduce the matrix by resin transfer moulding. For this reason it was necessary to avoid a flow constriction in the middle of the working section, so the cross weaving was carried out at two positions, 50mm either side of the centre line, where the cross sectional area was increasing. In a full-scale production flexbeam it might well be necessary to provide additional reinforcement in the region where the distance between the rods is increasing, however this was not thought necessary for this prototype.

Manufacture of mould tooling and moulding of demonstrator.

The mould was cast from epoxy resin filled with aluminium powder using a half thickness master model mounted on a mould board at the required parting line. The two half mould faces were cast within aluminium cages to which were attached the cup and cone alignment features, clamping and jacking features were also mounted on this frame. The tool was completed by machining a groove for an 'O' ring seal, and drilling resin in and out ports. The tool was unheated and was used within an oven for the final component cure. For the prototype mouldings a modified formulation was used so that a somewhat lower embedding matrix modulus (approx 320MPa) could be achieved, coupled with a lower mixed viscosity for ease of injection. The formulation was 39% CY219 epoxy, 39% Trixene B1770, 22% CY219 hardener, the CY219 epoxy resin has a very low initial viscosity compared to the MY750 DGEBA resin used in earlier trials. For the prototype mouldings the formulated epoxy/polyurethane blend was introduced into two in-gates at one end of the tool at a pressure of up to 70kN, whilst drawing a vacuum from a port at mid length and the two ports at the other end of the tool. Only a low positive pressure was used on the resin pot, with much of the driving force being supplied by the applied vacuum. This was done to avoid disturbing the rod positions. The port at mid length was closed when the resin reached it. The vacuum was shut off at about two thirds full and the remaining injection was under pressure only conditions. The injection was stopped when clear resin was seen to be emerging from the out gates.

Testing of the demonstrator

The demonstrator was tested in torsion using an Avery Dennison 6609 CGG torsion machine. Fig 12 shows the sample in the test machine with a 20^0 twist applied. Fig 13 shows the torque/twist curve.

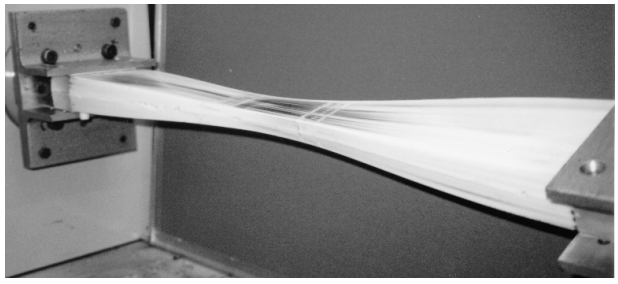

Fig 12. Prototype flexbeam element undergoing torsion testing.

The predicted torsional stiffness (from FEA) was 3.26Nm/degree at small deflections. The measured torsional stiffness was 3.2Nm/degree at 2^0 twist, falling to 2.3Nm/degree at 20^0 twist. The prototype snapped back to the undeformed shape when the load was removed with no permanent set or apparent damage.

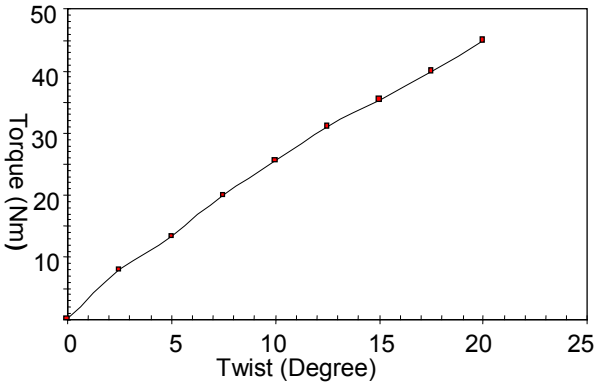

Fig 13. Torque versus twist curve for prototype flexbeam element

Discussion and Conclusions

The materials and processing requirements for the design of a bearingless main rotor for a heavy helicopter are very severely constrained by the loading and use environment, whatever approach is being taken. The use of conventional composite materials has proven to be intractable and the approach described here is an attempt to develop an alternative that opens out the design possibilities.

Composites of extreme anisotropy can be designed to have a specific suite of properties in torsion and bending. The key to achieving high bending to shear stiffness ratios, whilst avoiding a reduction in compressive strength due to fibre microbuckling, lies in the use of pre-cured carbon fibre reinforced rods which have an inherent resistance to buckling. These rods are then introduced into a matrix of carefully designed stiffness to provide the proper balance of support and flexibility.

The properties of samples manufactured with various embedding matrices have been measured, and the concept of embedding rods in a matrix of controlled stiffness has been shown to be a valid route to the generation of composites of very high and controlled levels of anisotropy. However, for a practical solution for applications such as a bearingless main rotor the properties of the materials must remain within acceptable limits over the whole of the operational temperature, humidity and chemical environment range. As the matrix stiffness property requirements fall into the range typical of polymers in the region of their T_g, there is a very clear prospect for difficulties with a solution based on the use of a simple, single phase, formulated matrix.

Acceptable solutions to the matrix requirements would fall into two classes, the T_g must be maintained either always above the operating temperature range or always below it. Attempts to produce a material with the correct mechanical properties and a high T_g by generating a foam did not meet with success, although this avenue is by no means exhaustively explored and solutions may be possible.

The first steps have also been taken towards the development of a route for the development of such components where the matrix T_g is below the operating temperature range. This approach uses an elastomeric embedding matrix. Additional stiffness is then provided by a small amount of well-directed aramid reinforcement. This approach has been shown to eliminate the torsional buckling mode that imposes one performance limit on rod-reinforced low modulus matrices. The test samples manufactured with a polyurethane elastomer embedding matrix proved to be remarkably robust in terms of their ability to recover from extreme deformations. If this robustness could be maintained, whilst the stiffness was augmented with properly directed reinforcement this approach would seem to have many benefits.

It is worthwhile to look more widely at the design freedoms inherent in the approach of embedding precured reinforcement rods in suitable matrices, as these go far beyond the simple geometries described above.

Fig 14, shows some of the available design freedoms in a schematic way. The reinforcing rods may be of different sizes, shapes and materials and can be distributed inside the space with a great deal of freedom. Modification to the component cross-sectional shape and area represent additional design freedoms for simple rod reinforced matrices.

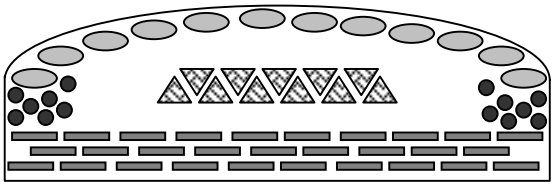

Fig 14. Schematic of design freedoms available with rod reinforced matrices.

As noted previously, the properties of such simple rod reinforced structures can be modified by the addition of a light external overwinding of aramid fibre at a suitable fibre orientation. Other

possibilities are to utilise an internal reinforcement, which might, for example, be an interweaving such as is shown in fig 15.

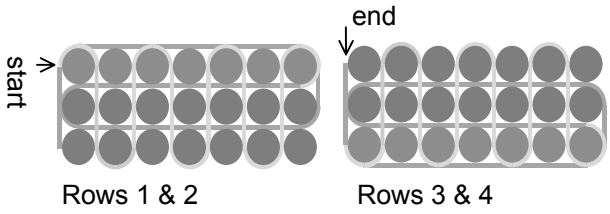

Fig 15. Additional design freedoms are available, such as interweaving of additional reinforcement.

Samples have been made in which an aramid interweave has been introduced at a volume fraction of just over 3% (without any change in the rod volume fraction). This gives an effective transverse modulus of about 4GPa, even if the embedding matrix modulus were essentially zero. Clearly a higher modulus could be achieved if the reinforcing rod packing were to be reduced and there is no necessity for through thickness and widthwise modulus to be identical.

Another design freedom may be achieved by bringing together groups of reinforcing rods and combining them into larger reinforcing elements, see fig 16. It has been shown (ref 12) that applying a tensioned hoop overwinding to a rod based composite can generate a radial precompression that has a major effect on the properties of the composite. For example, the overwinding almost eliminates the sensitivity to impact in a rod-reinforced bar using a brittle epoxy embedding matrix. Hoop overwinding on an elastomer matrix rod-reinforced composite would greatly increase the effective transverse stiffness and tend to suppress any deformatiion modes that lead to an increase in cross-sectional area.

To date the approach of using a simple formulated matrix has been used in the design, manufacture and test of a sub-scale demonstrator component based on the requirements of a bearingless main rotor for a heavy helicopter. Techniques have been developed for handling the rods and assembling them into a structure and for terminating them into a metallic end fitting. Samples have been manufactured using resin transfer moulding techniques in simple tooling. The initial stiffness of a demonstrator component has been measured at a value very close to that arrived at by FEA techniques.

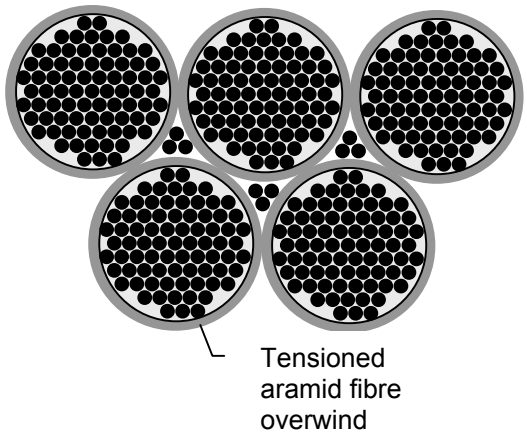

Fig 16. Groups of rods can be brought together to give an additional design freedom

Future directions will involve the investigation of the design freedoms that are inherent in the approach of using precured rods. Despite the additional complexity that will arise from using an embedding matrix with a T_g below the operating temperature range, this is seen as being a better long-term option that trying to formulate a material of low modulus, high T_g and acceptable processing characteristics. With development the target of producing a flexbeam for a bearingless main rotor of a heavy helicopter is seen as achievable.

Acknowledgement

The authors would like to acknowledge the support of the Engineering and Physical Sciences Research Council for this research under contract number GR/K66833, and to acknowledge the input of Carl Tharme for his work on finite element analysis, Laurence Vaughn for his work on the manufacture of demonstrator components and Antonio Gonzalez Sanchez for his work on the testing of pin-ended compression specimens.

References.

1. US Patent 4332525, Matched stiffness flexbeam and blade system, June 1981.
2. US Patent 4648800, Composite flexbeam for a rotary wing aircraft, March 1987
3. US Patent 5096380, Composite flexbeam for a bearingless helicopter rotor, March 1992
4. US Patent 5738494, Optimised composite flexbeam for helicopter rotors, April 1998
5. Niwa. Y., & Bandoh. S., Study of bearingless rotor hub system for XOH-1, 54th Annual Forum of the American Helicopter Society, April 1998.

6. Enenll. B., & Kloeppel. V., Design verification and flight testing of a bearingless soft inplane tail rotor. 11th European Rotorcraft Forum, London, Sept 1985.
7. Fish. J., & Vizzini. A., Tailoring concepts for improved structural performance of rotorcraft flexbeams. Composites Engineering. Vol 2 5/7 pp 303-312 1992.
8. Murri. G., O'Brien. T., & Rousseau. C., Fatigue life methodologies for tapered composite flexbeam laminates. 53rd Annual Forum of the American Helicopter Society, Virginia Beach, April 1997.
9. AB Clarke, MR Wisnom, KD Potter. Development and verification of standard test methods for small diameter unidirectional carbon/epoxy rods. Proc ECCM CTS4. Lisbon. August 1998.
10. MR Wisnom, & KD Potter, Unidirectional carbon fibre rods for high performance structures Designing High Performance Stiffened Structures: IMechE, June 1999. Institution of Mechanical Engineers, 1999.
11. A Towse, CJ Setchell, KD Potter, AB Clarke, JHG Macdonald, MR Wisnom, & RD Adams, Use experience with a developmental general purpose non-contacting extensometer with high resolution. American Society for Testing and Materials (Special Technical Publication): Non-traditional methods of sensing stress, strain and damage in materials and structures.. STP 1323 ASTM (2001) (Paper ID 8209)
12. KD Potter. F Schweikhardt & MR Wisnom. Impact response of unidirectional carbon fibre rod elements with and without an impact protection layer. J. Composite Materials, 34/17/2000 1437 - 1455